Scientific Journal Impact Factor: 3.762

e- ISSN: 2394-5532
p- ISSN: 2394-823X

International Journal of Applied And Pure Science and Agriculture

www.ijapsa.com

Performance of blood flow through two phase stenosed artery using Herschel-Bulkley model

Sapna Ratan Shah, S.U. Siddiqui and Anuradha Singh

Department of Mathematics, Harcourt Butler Technological Institute,
Kanpur - 208002, (India) Fax No.0512-2533812,

Abstract

This paper presents the study of blood flow through stenosed artery by assuming the blood as a two fluid model with the suspension of all the erythrocytes in the core region as a non-Newtonian fluid and the plasma in the peripheral layer as a Newtonian fluid. The non-Newtonian fluid in the core region of the artery is assumed as a Herschel-Bulkley fluid. Perturbation technique is used to obtain the analytic expression for wall shear stress, plug core radius, volumetric flow rate, and velocity profile. The blood flow velocity deviates with the various parameter such as shape of stenosis, non- Newtonian behavior parameter, radius of plug core ɵ, A, z and time etc. and this deviation of flow velocity can be reregulated by a proper use of model. It is found that the blood velocity decreases with the radial distribution for any given value of m. The ultimate numerical solution of the flow rate and wall shear stress for different values of blood flow characteristics (n, m, r, ɵ, δ, A) are discussed through the graph. The physical interpretation of obtain expression is shown in the present paper for the better understanding of the problem and in biomedical and bioengineering field.

Key words: Stenosed artery, non-Newtonian, Herschel-Bulkley fluid, Flow rate, velocity profile.

I. INTRODUCTION

The cardiovascular diseases have been notice as one of the major illness where numerous peoples suffer from them. The cardiovascular system consists of the heart and blood vessels which play an important role in the transportation protection and regulation of human body. A pressure gradient produces as a heart pump so that blood will flow through the blood vessels in the body [3]. At present, a considerable attention has been noticed in the study of blood flow through stenosed or constricted arteries. An abnormal growth reducing the lumen of an artery is usually called stenosis or atherosclerosis which is a wide spread cardiovascular disease [2]. Arteries are clear pipes and blood can flow easily through them, but sometimes due to such unfamiliar growth, there is caused serious circulatory disorders by reducing or occluding the blood supply. Stenosis developed in arteries supplying blood to brain, can bring about cerebral strokes, likewise in coronary arteries, it can cause myocardial infarction, leading to heart failure. The wall shear stress and resistance to flow are physiologically important quantities which play an important role in the formation of platelets [17]. High wall shear stress not only damages the vessel wall and causes intimal thickening but also activates platelets, causes platelet aggregation, and finally results in the formation of thrombus [3]. In 1968, Young [22] has presented a mathematical model to analyze the effects of stenosis on the flow characteristics of blood. It is concluded that resistance to flow and wall shear stress increase with an increase in stenosis size. Blood flow models with axially symmetric stenoses are considered by many authors [2, 5, 9, 13, and 15]. In 2010, Singh et al. [16] have dealt blood flow model through radially non-symmetric stenosed artery. In 2008, Radhakrishnamcharya and Prasad have proposed blood flow through an inclined tube with an stenosis. Recently in 2012, Kumar et al. [10] have proposed two layered model of blood flow with porous effect. Several theoretical and experimental attempts [1, 6, 17, 19, and 21] were made to study the blood flow characteristics in the presence of stenosis. The assumption of Newtonian behavior of blood is acceptable for high shear rate flow through larger arteries. But blood, being a suspension of cells in plasma, exhibits non-Newtonian behavior at low shear rate ($\gamma < 10/sec$) in small diameter arteries [1, 22].

In diseased state, the actual flow is distinctly pulsatile. Many researchers [4, 7, 8, 18, and 20] studied the non-Newtonian behavior and pulsatile flow of blood through stenosed arteries. Bugliarello and Sevilla [2] have shown experimentally that for blood flowing through narrow blood vessels, there a peripheral layer of plasma and a core region of suspension of all the erythrocytes. Thus, for a realistic description of the blood flow, it is appropriate to treat blood as a two-fluid model with the suspension of all the erythrocytes in the core region as a non-Newtonian fluid and plasma in the peripheral region as a Newtonian fluid. In 2005, Mandal [11] reported that Casson fluid model and Herschel-Bulkley fluid model are the fluid models with nonzero yield stress and they are more suitable for the studies of the blood flow through narrow arteries. It has been reported by Mathur [12] that Casson fluid model is simple to apply for blood flow problems, because of the particular form of its constitutive equation, whereas, Herschel-Bulkley fluid model's constitutive equation is not easy to apply because of the form of its empirical relation, since, it contains one more parameter than the Casson fluid model. Thus, in this paper, we extend this study to two-fluid Herschel-Bulkley model, Newtonian fluid model and compare these models and discuss the advantages of the two-fluid model.

II. FORMULATION OF THE PROBLEM:

Let us consider an axially symmetric, laminar, pulsatile and fully developed flow of blood through a circular artery having a stenosis (Fig. 1). Cylindrical polar coordinate($r^*, \emptyset^*, z^*$), with the pole located on the axis of the artery have been used to analyze the problem.

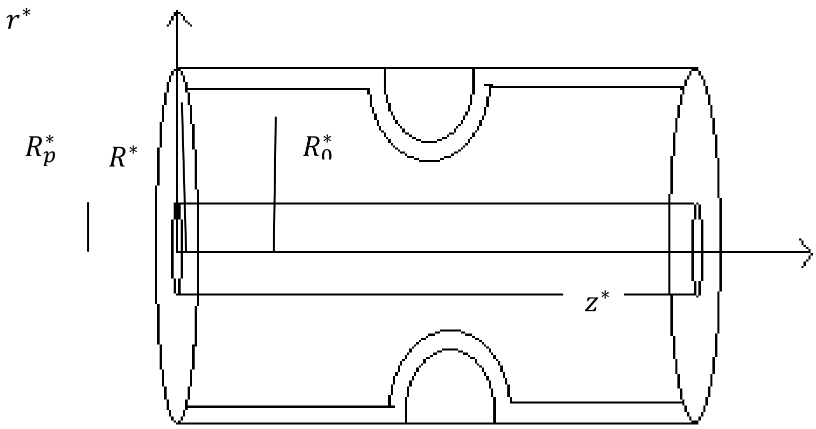

Fig. 1. Schematic diagram of multiphase blood flow in a stenosed artery

The momentum equation is given by

$$\rho \frac{\partial u^*}{\partial t^*} = -\frac{\partial p^*}{\partial z^*} - \frac{1}{r^*}\frac{\partial (r^* \tau^*)}{\partial r^*} \quad (1)$$

The Harshes Bulkly equation describing the non-Newtonian behavior of blood may be written as

$$-\frac{\partial u^*}{\partial r^*} = \frac{1}{\mu}(\tau - \tau_0)^{1/n}, \qquad \tau^* > \tau_y \quad (2)$$

$$-\frac{\partial u^*}{\partial r^*} = 0, \qquad \tau^* \le \tau_y \quad (3)$$

The theoretical analysis takes care of the two-phase flow of blood, the peripheral plasma layer is considered to be Newtonian, while the core region that is supposed to contain all the erythrocytes contained in the blood inside the artery is treated as non-Newtonian. The mathematical model that is developed here is formulated by the following set of equations:

$$\tau^* = -\mu \frac{\partial u^*}{\partial r^*}, \qquad if\ R_0^*(z^*, t^*) < r^* < R^*(z^*, t^*), \quad (4)$$

$$-\frac{\partial u^*}{\partial r^*} = \frac{1}{\mu}(\tau - \tau_0)^{1/n}, \qquad if\ R_p^*(z^*, t^*) < r^* < R_0^*(z^*, t^*), \quad (5)$$

$$-\frac{\partial u^*}{\partial r^*} = 0, \qquad if\ 0 < r^* < R_p^*(z^*, t^*) \quad (6)$$

Along with the boundary conditions

$u^* = 0$ at $r^* = R^*(z^*, t^*)$, (7)

τ^* is finite at $r^* = 0$. (8)

These equations are to be supplemented by the condition of continuity of u^* and r^* at the interfaces $r^* = R_0^*(z^*, t^*)$and $r^* = R_p^*(z^*, t^*)$.

The pressure gradient which is function of z^* and t^*, is represented as

$$\frac{\partial}{\partial z^*} p^*(z^*, t^*) = -q^*(z^*) f(t^*)$$

with $q^*(z^*) = -\frac{\partial}{\partial z^*} p^*(z^*, 0), f(t^*) = 1 + A\sin(\omega t^*)$.

For the analysis presented in the sequel, we use the following non-dimensional variables

$$z = \frac{z^*}{a}, r = \frac{r^*}{a}, R(z,t) = \frac{R^*(z^*,t^*)}{a}, R_0(z,t) = \frac{R_0^*(z^*,t^*)}{a}, \quad R_p(z,t) = \frac{R_p^*(z^*,t^*)}{a}, \tau = \frac{2\tau^*}{q_0 a}, \quad \theta = \frac{2\tau_y}{q_0 a}, u = \frac{u^*}{\frac{q_0 a^2}{4\mu}}, t = t^*\omega, Q(z,t) = \frac{Q^*(z,t)}{\frac{\pi q_0 a^4}{8\mu}}, d = \frac{d^*}{a}, \ \delta = \frac{\delta^*}{a}, L_0 = \frac{L_0^*}{a}, L = \frac{L^*}{a}, \alpha^2 = \frac{\alpha^2 \omega}{\frac{\mu}{\rho}}, q(z) = \frac{q^*(z^*)}{q_0} \quad (9)$$

where q_0 is the constant pressure gradient (which is negative).

In terms of these non-dimensional variables, eq. (1) reads

$$\alpha^2 \frac{\partial u}{\partial t} = 4q(z)f(t) - 2\frac{1}{r}\frac{\partial(r\tau)}{\partial r}, \qquad 0 < r < R(z,t), \tag{10}$$

while the equations (2) to (6) take the forms

$$-\frac{\partial u}{\partial r} = 2\tau, \qquad R_0(z,t) < r < R(z,t), \tag{11}$$

$$-\frac{\partial u}{\partial r} = 2(\tau-\theta)^n, \qquad R_p(z,t) < r < R_0(z,t), \tag{12}$$

$$-\frac{\partial u}{\partial r} = 0, \qquad 0 < r < R_p(z,t), \tag{13}$$

u=0 at r=R, τ is finite at r=0.

Also u and τ have to be continuous at $r = R_0(z,t)$ and $r = R_p(z,t)$. The geometry of the stenosis in non-dimensional form is given by

$$R(z,t) = \begin{cases} 1 - A_1(t)\left[L_0^{(m-1)}(z-d) - (z-d)^m\right], & if\ d \le z \le d + L_0, \\ 1, & \text{otherwise} \end{cases}$$

with

$$A_1(t) = \frac{\delta[1-e^{(-t/T)}]m^{\frac{m}{m-1}}}{aL_0^m(m-1)}, \quad m \neq 1$$

here δ denotes the maximum height of the stenosis. The maximum height being attained at $z = d + L_0/m^{1/(m-1)}$. The volumetric flow rate is given by
$Q(z,t) = 4\int_0^{R(z,t)} \tau u(z,r,t)dr.$

III. Analytical solution of the problem

Considering the Womersley parameter to be very small, the velocity u, shear stress τ as well as R_0 and R_p can be expressed in the following form

$u(z, r, t) = u_0(z, r, t) + \alpha^2 u_1(z, r, t) + \dots$ (14)
$r(z, r, t) = r_0(z, r, t) + \alpha^2 u_1(z, r, t) + \dots$ (15)
$R_0(z, r, t) = R_{00}(z, r, t) + \alpha^2 R_{10}(z, r, t) + \dots$ (16)
$R_p(z, r, t) = R_{0p}(z, r, t) + \alpha^2 R_{1p}(z, r, t) + \dots$ (17)
Using (14) and (15) in (10). we have

$$\frac{\partial}{\partial r}(r\tau_0) = 2rq(z)f(t) \tag{18}$$

$$\frac{\partial u_0}{\partial t} = -\frac{2}{r}\frac{\partial}{\partial r}(r\tau_1) \tag{19}$$

Integrating (18) and using the boundary condition, we have

$$\tau_0 = q(z)f(t)R_p, \qquad 0 \le r \le R_p. \tag{20}$$

In the regions $R_p \le r \le R_0$ and $R_0 \le r \le R$, the continuity of τ_0 at R_{0p} and R_{00} yield

$$\tau_0 = q(z)f(t)r. \tag{21}$$

Introducing (14) and (15) into equations (11) to (13) and equating like powers of α we obtain

$$-\frac{\partial u_0}{\partial r} = 2\tau_0, \quad -\frac{\partial u_1}{\partial r} = 2\tau_1, \quad \text{if } R_0 \le r \le R. \tag{22}$$

$$-\frac{\partial u_0}{\partial r} = 2\left[(-\theta)^n + n\tau_0(-\theta)^{(n-1)} + \frac{n(n-1)}{2}\tau_0^2(-\theta)^{(n-2)} + \frac{n(n-1)(n-2)}{6}\tau_0^3(-\theta)^{(n-3)} + \dots\right]$$

$$-\frac{\partial u_1}{\partial r} = 2\left[n\tau_1(-\theta)^{(n-1)} + \frac{n(n-1)}{2}\tau_0\tau_1(-\theta)^{(n-2)} + \frac{n(n-1)(n-2)}{6}3\tau_0^2\tau_1(-\theta)^{(n-3)} + \cdots\right]$$
$$\text{if } R_p \le r \le R_0 \tag{23}$$

$$\frac{\partial u_0}{\partial r} = 0, \quad \frac{\partial u_1}{\partial r} = 0 \quad \text{if } 0 \le r \le R_p. \tag{24}$$

The boundary condition for u_0 and u_1 are:
$u_0 = 0$, $u_1 = 0$ at $r = R$ (25)
u_0 , u_1 are continuous at R_{00} and R_{0p}.
from (21), (22) and (25) we have

$$u_0 = q(z)f(t)(R^2 - r^2) \qquad R_0 \le r \le R \tag{26}$$

using (25) in (21) and (23), one can find

$$u_0 = \left[(-\theta)^n(R_{00} - r) + \frac{n}{2}q(z)f(t)(R_{00}^2 - r^2)(-\theta)^{(n-1)} + \frac{n(n-1)}{6}\big(q(z)f(t)\big)^2(R_{00}^3 - r^3)(-\theta)^{(n-2)}\right] + q(z)f(t)(R^2 - R_{00}^2)$$
$$R_p \le r \le R_0 \tag{27}$$

Now from (21), (24), (25) and (27)

$$u_0 = 2\left[(-\theta)^n\big(R_{00} - R_{0p}\big) + \frac{n}{2}q(z)f(t)\big(R_{00}^2 - R_{0p}^2\big)(-\theta)^{(n-1)} + \frac{n(n-1)}{6}\big(q(z)f(t)\big)^2\big(R_{00}^3 - R_{0p}^3\big)(-\theta)^{(n-2)}\right] + q(z)f(t)(R^2 - R_{00}^2)$$
$$0 \le r \le R_p \tag{28}$$

Neglecting the squares and higher power of α in (17) and using (20), one obtains

$$r|_{\tau_0=\theta} = R_{0p} = \frac{\theta}{q(z)f(t)}. \qquad (29)$$

Again, making use of the regularity condition that τ_1 is finite at r = 0, equation (28) along with (19) gives

$$\tau_1 = -\left[(-\theta)^n(R_{00} - R_{0p}) + \frac{n}{2}q(z)f'(t)(R_{00}^2 - R_{0p}^2)(-\theta)^{(n-1)} + \frac{n(n-1)}{3}(q(z))^2 f(t)f'(t)(R_{00}^3 - R_{0p}^3)(-\theta)^{(n-1)} + \cdots\right]R_{0p} - q(z)f'(t)(R^2 - R_{00}^2)\frac{R_{0p}}{4} \qquad 0 \le r \le R_p$$

The continuity of τ_1 at r = R_{0p} yields

$$\tau_1 = -\left[(-\theta)^n\left(R_{00}\frac{r}{2} - \frac{r^2}{3}\right) + \frac{n}{2}q(z)f'(t)\left(R_{00}^2\frac{r}{2} - \frac{r^3}{4}\right)(-\theta)^{(n-1)} + \frac{n(n-1)}{3}(q(z))^2 f(t)f'(t)\left(R_{00}^3\frac{r}{2} - \frac{r^4}{5}\right)(-\theta)^{(n-1)} + \cdots\right] - q(z)f'(t)(R^2 - R_{00}^2)\frac{r}{4} + \frac{A_2}{r} \qquad R_p \le r \le R_0$$

The expression for A_2 is given in the Appendix.

Similarly, since τ_1 is continuous at R_0, we have

$$\tau_1 = \frac{1}{2}q(z)f'(t)\left(R^2\frac{r}{2} - \frac{r^3}{4}\right) + \frac{A_3}{r} \qquad R_0 \le r \le R,$$

Where A_3 stands for a quantity whose expression is presented in the Appendix.

Using (25), the equations (22)-(24) give rise to

$$u_1 = -q(z)f'(t)\left[\frac{R^2}{4}(R^2 - r^2) - \frac{(R^4 - r^4)}{16}\right] - A_3\log\left(\frac{r}{R}\right) \qquad R_0 \le r \le R$$

$$u_1 = X(r) \qquad R_p \le r \le R_0$$

$$u_1 = X(R_{0p}) \qquad 0 \le r \le R_p$$

Where,

$$A_2 = -\left[(-\theta)^n\left(R_{00}\frac{R_{0p}}{2} - \frac{2}{3}R_{0p}^2\right) + \frac{n}{2}q(z)f'(t)\left(R_{00}\frac{R_{0p}}{2} - \frac{3}{4}R_{0p}^3\right)(-\theta)^{(n-1)} + \frac{n(n-1)}{3}(q(z))^2 f(t)f'(t)\left(R_{00}^3\frac{R_{0p}}{2} - \frac{4}{5}R_{0p}^4\right)(-\theta)^{(n-2)} + \cdots\right]R_{0p}$$

$$A_3 = -\left[(-\theta)^n\left(\frac{R_{00}^2}{6}\right) + \frac{n}{2}q(z)f'(t)\left(\frac{R_{00}^3}{4}\right)(-\theta)^{(n-1)} + \frac{n(n-1)}{3}\big(q(z)\big)^2 f'(t)f(t)\frac{3}{10}R_{00}^4(-\theta)^{(n-2)} + \cdots\right]R_{00} - q(z)f'(t)\frac{R_{00}^2}{4}\left(\frac{2}{3}R^2 - \frac{3}{4}R_{00}^2\right) + A_2$$

$$X(r) = 2\Bigg[n(-\theta)^{(n-1)}\Bigg[(-\theta)^n\left(\frac{R_{00}}{4}(r^2 - R_{00}^2) - \frac{1}{9}(r^3 - R_{00}^3)\right) + \frac{n}{2}q(z)f'(t)(-\theta)^{(n-1)}\left(\frac{R_{00}^2}{4}(r^2 - R_{00}^2) - \frac{1}{16}(r^4 - R_{00}^4)\right) + \frac{n(n-1)}{3}\big(q(z)\big)^2 f'(t)f(t)(-\theta)^{(n-2)}\left(\frac{R_{00}^3}{4}(r^2 - R_{00}^2) - \frac{1}{25}(r^5 - R_{00}^5)\right) + \cdots\Bigg] + q(z)f'(t)(R^2 - R_{00}^2)\frac{(r^2 - R_{00}^2)}{8} - A_2 log\left(\frac{r}{R}\right) + \frac{n(n-1)}{2}q(z)f(t)(-\theta)^{(n-2)}\Bigg[(-\theta)^n\left(\frac{R_{00}}{6}(r^3 - R_{00}^3) - \frac{1}{12}(r^4 - R_{00}^4)\right) + \frac{n}{2}q(z)f'(t)(-\theta)^{(n-1)}\left(\frac{R_{00}^2}{6}(r^3 - R_{00}^3) - \frac{1}{20}(r^5 - R_{00}^5)\right) + \frac{n(n-1)}{3}\big(q(z)\big)^2 f'(t)f(t)(-\theta)^{(n-2)}\left(\frac{R_{00}^3}{6}(r^3 - R_{00}^3) - \frac{1}{30}(r^6 - R_{00}^6)\right) + \cdots\Bigg] + q(z)f'(t)(R^2 - R_{00}^2)\frac{(r^3 - R_{00}^3)}{13} - A_2(r - R_{00})\Bigg]$$

The expression for velocity in the peripheral and core layers can now be calculated by using the equations (14), (26)-(28) and (30).

We note that yield plane, which was initially located at r = R_{0p} will be displaced by a distance $\alpha^2 R_{1p}$. The new location of the yield plane can be described mathematically by the equation

$$\tau^2\left(R_{0p} + \alpha^2 R_{1p}\right) = \theta^2$$

Expending it in Taylor's series about R_{0p} and using $\tau_0(R_{0p}) = \theta$, we have

$$R_{1p} = -\frac{\tau_1(R_{0p})}{p(z)f(t)} = -\frac{1}{p(z)f(t)}\Big[(-\theta)^n\big(R_{00} - R_{0p}\big) + \frac{n}{2}q(z)f'(t)\big(R_{00}^2 - R_{0p}^2\big)(-\theta)^{(n-1)} + \frac{n(n-1)}{3}[q(z)]^2 f(t)f'(t)\big(R_{00}^3 - R_{0p}^3\big)(-\theta)^{(n-2)} + \ \ldots\Big] \qquad (30)$$

Using (17), (29) and (30) we have the expression for R_p as

$$R_p = \frac{1}{q(z)f(t)}\theta + \alpha^2 \frac{1}{q(z)f(t)}\Big[\Big[(-\theta)^n(R_{00} - R_{0p}) + \frac{n}{2}q(z)f'(t)(R_{00}^2 - R_{0p}^2)(-\theta)^{(n-1)} + \frac{n(n-1)}{3}(q(z))^2 f(t)f'(t)(R_{00}^3 - R_{0p}^3)(-\theta)^{(n-2)} + \cdots\Big] R_{0p} + q(z)f(t)(R^2 - R_{00}^2)\frac{R_{0p}}{4}\Big] \quad (31)$$

The volumetric flow rate can be computed from (18) by re-writing it in the form

$$Q(z,t) = 4\left(u(z,R_p,t)\frac{R_p^2}{2} + \int_{R_p}^{R_0} ru(z,r,t)dr + \int_{R_0}^{R} ru(z,r,t)dr\right). \quad (32)$$

Different expression for u(z, r, t) can to be used for the different regions.

The value of the wall shear stress τ_ω is a quantity that is of particular importance from the physiological point of view. It is given by

$$\tau_\omega = (\tau_0 + \alpha^2\tau_1)|_{r=R} = q(z)f(t) + \alpha^2(-\frac{1}{2}q(z)f'(t)\left(\frac{R^3}{12}\right) + \frac{1}{R}A_3) \quad (33)$$

The value of R_{00} in (16) is found by using the continuity of u_0 at R_{00}. In doing so. We have used the Newton-Raphson method, by taking the non-dimensional velocity in the peripheral layer at R_{00} as its value in the steady case, i.e. 0.03. In the order to determine the value of R_{10}, we consider the equation

$$\tau^2(R_{00} + \alpha^2 R_{10}) = \tau_0^2(R_{00}).$$

The value of R_{10} can be obtained by expanding the left side of (25) in the Taylor's series about R_{00}.

It may be noted that if we write $u = u_0 + \alpha^2 u_1$ and use (26)-(28) and (30).

$$q(z) = \frac{Q_s}{R^4} + \frac{16}{7}\left(\frac{\theta Q_s}{R^5}\right)^{\frac{1}{2}} + \frac{64\theta}{49R}, \text{ where } R = R(z,t). \quad (32)$$

while computing q(z), one may take $Q_s = 1.0$.

IV. RESULTS AND DISCUSSION

The volumetric flow rate and the wall shear stress are the two important characteristics in the study of fluid flow through a stenosed artery. Using appropriate boundary conditions, analytical expressions for the velocity profile, volumetric flow rate and shear stress have been obtained. The expressions for volumetric flow rate and wall shear stress, given by (32) and (33) respectively have been numerically evaluated using MATLAB software for different values of relevant parameters. Estimates of the shear stress and the percentage of increase in the shear stress of the two-fluid Herschel-Bulkley model with n for different stenosis heights and length are presented graphically. For the purpose of numerical computation of the quantities of interest, we have performed a thorough quantitative analysis, by taking the following values of the different parameters involved in the present study:
$a = 0.5mm$, $L = 30$, $L_0 = 10$, $d = 10$, $\theta = 0.05$, $A = 0.7$, $\delta = 0.1$, $\alpha^2 = 0.049$, $m = 2.0$, $T = 1.0$.

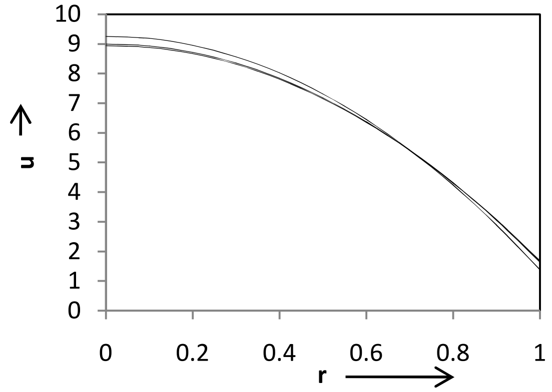

Fig. 2. Radial distribution of blood velocity at different shape of stenosis

Figs.2-3 depicts the effects of velocity of blood in the radial direction at different axial positions and at different instants of time. It can be observed that the blood velocity decreases as radius in plug flow region increases. It is also seen that blood velocity decreases as increases and further that the velocity decreases as the axial distance z increases from the onset of the stenosis up to the peak of stenosis. These results agree with the previous results obtained by Gupta et al. [6], Srivastava [20], and Radhakrishnamacharya and Prasad [14].

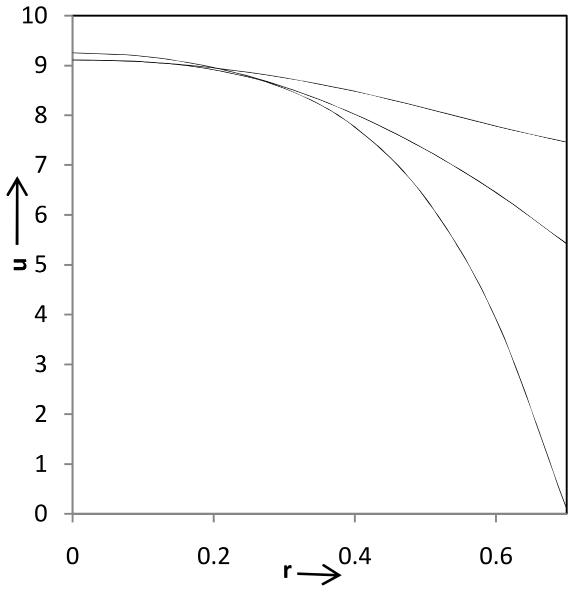

Fig. 3. Radial distribution of blood velocity at different values of n

The variation of the radius in the plug region of the stenosed portion is illustrated in Fig. 4-5, for the particular values of the amplitude (A) and the yield stress (θ). These figure shows that at a particular axial distance, as the value of δ (the height of the stenosed at t=0) increases, the radius of the plug flow zone decreases. Fig. 6-7 shows that variation of volumetric flow rate with time for different values of A and θ. These figures show that at all instant of time, the volumetric flow rate increases with the increase in amplitude and yield stress. Fig. 8 shows that variation of wall shear stress with z for different values of time. This figure shows that in the stenosed portion of the artery, the wall sheare stress increases with the increase in axial distance and also that at a given distance, it increases with the passage of time.

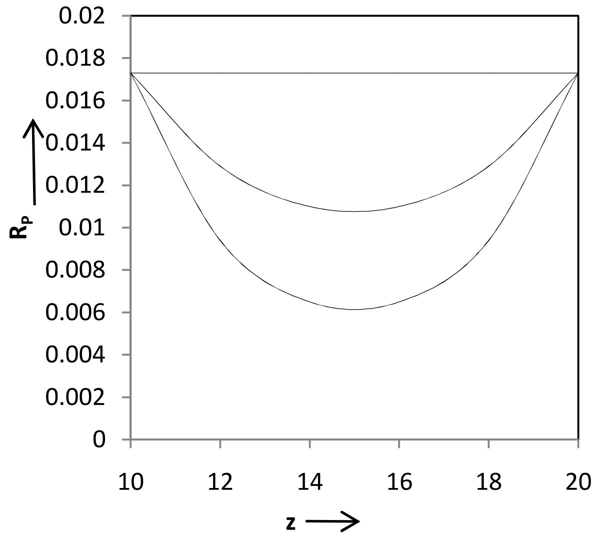

Fig. 4. variation of radius of plug core layer with z for different values of A, θ and δ

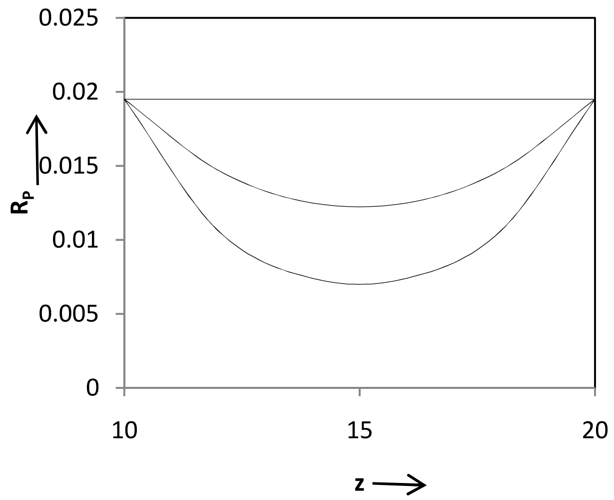

Fig. 5. variation of radius of plug core layer with z for different values of A, θ and δ

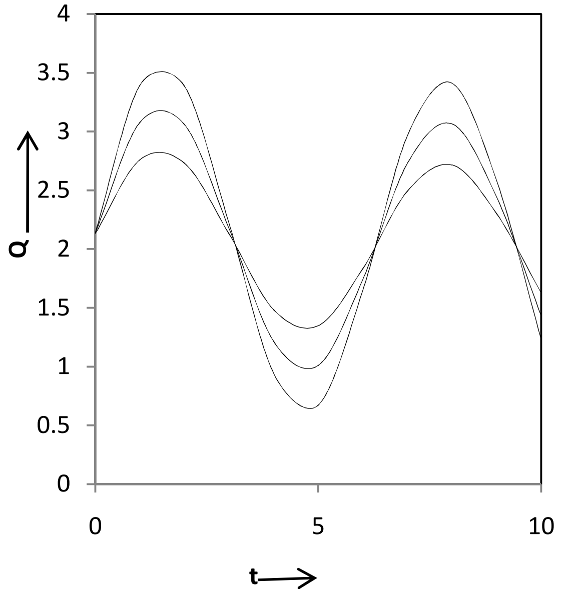

Fig. 6. variation of volumetric flow rate with time for different values of A

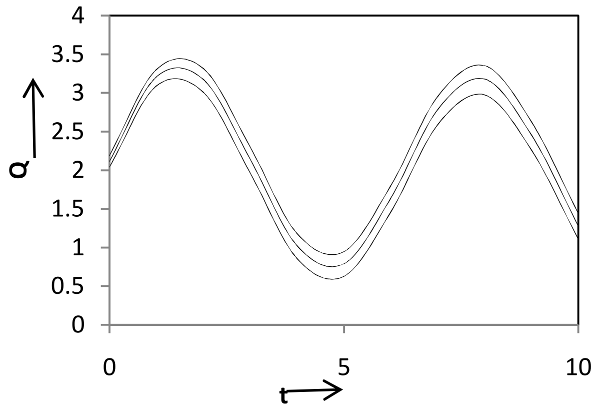

Fig. 7. variation of volumetric flow rate with time for different values of θ

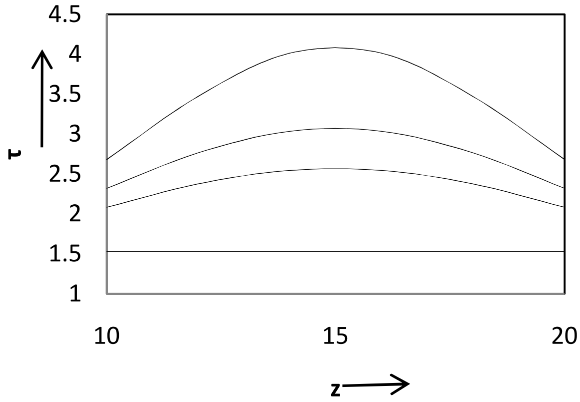

Fig. 8. Variation of wall shear stress with z for different values of time

V. Conclusion

From the above discussion, it is clear that the ratio of maximum height of stenosis and radius of normal artery and shear stress of the non-Newtonian fluid are strong parameter in fencing the blood flow. In this study it is obtained that the blood velocity decreases with the radial distribution for any given value of m. It is also found that the plug flow velocity and velocity distribution of the two-fluid non- Newtonian Herschel-Bulkley model are considerably higher than those of the two fluid Newtonian fluid models. It is also observed that the pressure drop, plug core radius, wall shear stress and the resistance to flow are significantly very low for the two-fluid non- Newtonian Herschel-Bulkley model than those of the two-fluid Newtonian fluid model. Hence, the two-fluid non- Newtonian Herschel-Bulkley would be more useful than the two-fluid Newtonian model to analyze the blood flow through stenosed arteries. Hence from all the above discussions we can conclude that a careful choice of the fluid model will affect the flow characteristics and can be utilized for medical and engineering applications.

BIBLIOGRAPHY

[1] Biswas, D., and Chakraborty, U. S., (2010), Two-Layered Pulsatile Blood Flow in a Stenosed Artery with Body Acceleration and Slip at Wall, Appl. Appl. Math., Vol. 3, pp. 1401-1418.
[2] Bugliarello, G. and J. Sevilla, (1970), Velocity Distribution and other Characteristics of Steady and Pulsatile Blood Flow in the Fine Glass Tubes, Biorheology, Vol. 17, pp. 85-107.
[3] Chakraborty, U. S., Biswas, D. and M. Paul, (2011), Suspension model blood flow through an inclined tube with an axially non-symmetrical stenosis. Korea-Australia Rheology Journal, Vol. 23, pp. 25-32.
[4] Chakraborty, U.S. D. Biswas, and M. Paul, (2011), Suspension model blood flow through an inclined tube with an axially non-symmetrical stenosis. Korea-Australia Rheology Journal, Vol .23, pp. 25-32.
[5] Dash, R. K., Jayaraman, G., and K. N. Mehta, (1999) “Flow in a catheterized curved artery with stenosis,” Journal of Biomechanics, Vol. 32, no. 1, pp. 49–61.
[6] Gupta, S. M., Gupta and S.P. Singh SP, (2012), Effect of radial viscosity variation on non-Newtonian flow of blood in a stenosed artery. International Journal of Applied Mathematics and Mechanics, Vol.8, pp. 51-61.
[7] Jain, N., Singh, S., and M. Gupta, (2012), Steady flow of blood through an atherosclerotic artery: A non-Newtonian model, International Journal of Applied Mathematics and Mechanics, Vol.8, pp. 52-63.
[8] Joshi, P., Pathak, A. and Joshi, B.K. (2009). Two-Layered Model of Blood Flow through Composite Stenosed Artery. Application and Applied Mathematics, Journal of Bio-Science and Bio-Technology. Vol. 3(1), pp. 27-38.

[9] Kandasamy, A. and Pai, R.G. (2013), Core Variation in the Entrance Region Flow of Casson Fluid in an Annuli. Applied Mechanics and Materials, Vol. 391, pp. 376-381.
[10] Kumar, A. Varshney C. L. and V.P. Singh, (2012), Performance Modelling and Study of blood Flow in Vessels with Porous Effects, Applied Mathematics, Vol. 2, pp. 166-170.
[11] Mandal, P. K., (2005) "An unsteady analysis of non-Newtonian blood flow through tapered arteries with a stenosis," International Journal of Non-Linear Mechanics, Vol. 40, no. 1, pp. 151–164.
[12] Mathur, P and Jain, S (2013): .Mathematical modeling of non-Newtonian blood flow through artery in the presence of stenosis., Applied Mathematical Biosciences, Vol. 4 (1), pp. 1-12.
[13] Ponalgoswami, R., (2007), Blood flow through an artery with mild stenosis: A Two-layered model, Different shapes of Stenoses and slip velocity at the wall, Journal of Applied Sciences, Vol .7, pp. 1071-1077.
[14] Radhakrishnamachariya, G and Prasad, K.M. (2008): .Flow of Herschel Bulkley fluid through an inclined tube of non-uniform crosssection with multiple stenosis., Arch. Mech,, Vol. 60 (2), pp. 161-172.
[15] Sarojamma and P. Nagarani, (2010), "Pulsatile flow of Casson fluid in a homogenous porous medium interface. Journal of the Indian Academy of Mathematics. 36(1), 167-185. International Journal of Application or Innovation in Engineering and Management. Vol .2 (12). pp. 30-41.
[16] Singh, B., Joshi, P. and B.K. Joshi, (2010), Blood flow through an artery having radially non-Symmetric mild stenosis, Appl. Math. Sci., Vol. 4, pp. 1065-1072.
[17] Srikanth, D, and Taddesse, K. (2012): .Mathematical analysis of non-Newtonian fluid flow through multiple stenotic artery in the presence of catheter- A pulsatile flow. International Journal of Nonlinear Science, Vol. 13 (1), pp. 15-27.
[18] Srivastava, V. P. and Rastogi, R. (2009): .Effect of hematocrit on impedance and shear stress during stenosed artery catheterization, Application and Applied Mathematics, Vol. 4,pp. 98- 113.
[19] Srivastava, V. P. and Rastogi, R. (2010): .Blood flow through stenosed catheterized artery: effect of hematocrit and stenosis shape. Comput. Math. Application, Vol. 59, pp. 1377-1385.
[20] Srivastava, V.P. (2000): .Particulate suspension blood flow through stenotic arteries: effect of hematocrit and stenosis shape. Indian Journal of Pure & Applied Mathematics, Vol. 33, pp. 1353-1360.
[21] Verma, N. and Parihar, R. S. (2010), Mathematical Model of Blood Flow Through a Tapered Artery with Mild Stenosis and Hematocrit, J. of Modern Mathematics and Statistics, Vol. 4, pp. 38-43.
[22] Young, D.F. (1968): .Effect of a time dependent stenosis on flow through a tube. J.Engg. for Ind., Trans of ASME, Vol.90, pp., 248-254.

